On the Operational, Shelf life and Degradation Mechanism in Polymer Field Effect Transistors

M. Javaid Iqbal[*1], Hamna Haq[1], Saira Riaz[1], M. Akram Raza[1], M. Zahir Iqbal[2], Mujeeb Ullah Chaudhry[3], Shahzad Naseem[1]

[1] Centre of Excellence in Solid State Physics, University of the Punjab, Quaid-e-Azam Campus, Lahore-54590, Pakistan

[2] Faculty of Engineering Sciences, GIK Institute of Engineering Sciences and Technology, Topi-23640, Khyber Pakhtunkhwa, Pakistan

[3] Department of Engineering, Durham University, Durham, DH1 3LE, United Kingdom

* Corresponding authors: javaid.cssp@pu.edu.pk (MJI); mujeeb.u.chaudhry@durham.ac.uk (MUC)

Abstract:

Organic Field Effect Transistors (OFETs) have shown great potential for future electronic technologies due to their low-cost solution processing, mechanical flexibility and potential applications for large area displays. One of the big obstacles in the realization of the practical applications is the inherent poor ambient stability of the OFETs. Here we report on the aging dependent degradation mechanism in the Poly[2,5-(2-octyldodecyl)-3,6-diketopyrrolopyrrole-alt-5,5-(2,5-di(thien-2-yl)thieno [3,2-b]thiophene)] (DPPDTT) based OFETs in the ambient conditions. These polymer OFETs showed the charge carrier mobility, threshold voltage and current on/off ratios in the range of 0.2 $cm^2V^{-1}s^{-1}$, -15V and 10^6 respectively. The device parameters showed variations in their values initially and then became stable with aging after ~20% initial degradations in the ambient. We have correlated the degradation in the OFET performance parameters with the degradation in the polymer channel layer that is confirmed with a time dependent FTIR spectra. Our findings are thus important to understand and achieve stability in OFET devices by aging them.

Introduction:

Organic Field Effect Transistors (OFETs) have acquired considerable importance because of the cost effectiveness, large area and flexible electronic device applications. The applications include flexible/bendable electronic displays, light emitting transistors, photo transistors, memory devices, radio frequency identification (RFID) tags, sensors etc. [1–6]. Recent progresses in organic semiconductors have shown immense potential for future electronic devices that can be assembled on flexible substrates, leading to new ways of developing organic electronics in many areas [7–10].

The remarkable improvements in both performance and reliability of OFETs suggest that they are competitive with existing inorganic semiconductor based devices [11]. A considerable progress has been made to enhance the mobility of the OFETs in the recent years [12,13], although the very recent literature have shown that the values are exaggeratedly over estimated in most of the cases [14–16]. Beside other issues, the major problems with the OFETs are their environmental and bias stress instabilities[17–19]. The stable operation is central in the realization of all practical applications offered by the OFETs. There are various reported reasons that contribute to the device instabilities. These include adsorption of water molecules [17,20,21], interface quality [22], oxidation [23,24], OFET channel length [25] and charge trapping in the dielectrics [26]. The general effect of instabilities results in the form of increase in the off-state current, decrease in the saturation current, decrease in the mobility, change in the threshold voltage and the on/off current ratios [17,19,20].

For all practical and active use of the devices, long shelf life and functional durability are required. Ambient atmospheric stability for long periods of time is one of the challenges for the devices having organic semiconductors as an active layer. Therefore consistent behavior of these parameters over time is essential for a stable durable OFET device.

Here, we show that it is possible to obtain the stable OFET operation by just aging the devices. In this work, we have studied the effect of storage time on the performance parameters of the Poly[2,5-(2-octyldodecyl)-3,6-diketopyrrolopyrrole-alt-5,5-(2,5-di(thien-2-yl)thieno [3,2-b]thiophene)] (DPPDTT) based OFETs. We prepared, stored and operated the OFET devices in the ambient environment. These solution-processed OFETs showed the effective charge career

mobility in the range of 0.2 $cm^2V^{-1}s^{-1}$, threshold voltage around -15V and current on/off ratio on the order of 10^6. A detailed analysis of the charge carrier mobility calculation is also provided to rule out the mobility overestimation or any other spurious effects. The FTIR spectrum was used to find out the reasons that caused the initial instabilities in the OFET devices and the films.

Experimental Details:

A bottom gate, top source drain contact devices (shown in **Fig. 1(a)**) were fabricated using commercially purchased highly doped n-type silicon substrates with pre-deposited 400 nm Si_3N_4 as the dielectric layer. Prior to the material deposition, the substrate surface was cleaned in warm acetone and then iso-propyl alcohol in an ultrasonic bath for 20 minutes each followed by blow dry with pressurized nitrogen. In order to remove the moisture molecules on the surface, the substrates were heated for 10 min at 100°C and then Poly(methyl methacrylate) (PMMA) (20mg/ml in chlorobenzene) was spun coated (1000 rpm, 60 sec.) as a second layer of the dielectric on top of 400nm Si_3N_4. The PMMA layers were then annealed at 150°C for 15 min. The solution processible organic polymer Poly[2,5-(2-octyldodecyl)-3,6-diketopyrrolopyrrole-alt-5,5-(2,5-di(thien-2-yl)thieno [3,2-b]thiophene)], (DPPDTT), (purchased from 1-Material) having a molecular weight, Mw~100,000 (PDI~3) was used for the channel material (**Fig. 1(b)**). The polymer solution was prepared by dissolving and magnetically stirring 13mg DPPDTT in 2ml chloroform at 800 rpm for 10 hours at 60°C. This solution of DPPDTT was then deposited onto the substrate by spin coating (1000rpm, 60 sec) and annealed in a furnace at 100°C for 20 minutes in 150 L/hr nitrogen gas flow. The source drain contacts were deposited by thermal evaporation of molybdenum oxide and gold through shadow mask (dimensions, L=120μm, W=3mm) in a thermal evaporation unit.

The electrical characterization of the devices was performed with Keithly 4200 SCS attached to a probe station. All the fabrication and characterization steps were performed at ambient air conditions except annealing of the PMMA and DPPDTT layers that was performed in 150L/hr nitrogen flow. For the FTIR analysis, Shimadzu ITTracer-100 was used in the ATR mode.

Results and Discussion:

The bottom gate top contact configuration OFET devices were fabricated and characterized in ambient conditions. **Fig. 1(a and b)** respectively show the device schematic and molecular structure of the DPPDTT. Typical transfer and output characteristics obtained are shown in **Fig. 1(c and d)** respectively. The device showed a typical p-type charge carrier behavior. The threshold voltage V_{th} was determined by linear extrapolation of the transfer curves [27]. The field effect mobility was extracted in the saturation regime [$V_{DS} > (V_G - V_T)$] from the slope of the square root of the source-drain current vs gate voltage (**Fig. 2(a)**) using the modified MOSFET equation [28]:

$$\mu_{sat} = \frac{2L}{C_i W}\left(\frac{d\sqrt{|I_{ds}|}}{dV_g}\right)^2 \qquad \textbf{(1)}$$

Where μ_{sat} is the field-effect carrier mobility in the saturation regime, C_i is the capacitance per unit area for the gate insulator which is 10nF/cm^2 in our case, W and L are channel width and length of the device respectively, I_{ds} is the drain-source current and V_g is the applied gate-to-source bias. The transfer curves showed two slopes for most of the curves obtained as shown in **Fig. 2(a)**. A slight hump was observed in the transfer curves, which is known to lead an overestimation of the mobility. The emergence of two slopes on a transfer curve that can contribute towards the gate voltage dependent mobility due to several factors, such as electron injection from the electrodes, contact resistance, mobility dependent on carrier density and non-equilibrium biasing of OFETs having short channels [13]. In account of these stated issues, mobility was calculated in the higher and lower slope regions of the transfer curves and on the full single slope on the entire transfer curve in the saturation regime as shown in the **Fig. 2(a)**. In order to take into account the spurious contributions and hence non-ideal behavior of the transfer curves, it was recently recommended to calculate the reliability factor and hence the effective mobility of the devices under study. The reliability factor in the saturation regime is given by the **equations (2) & (3),** where, L, W, Ci and μ_{sat} are the channel length, width, gate capacitance per unit area and calculated (claimed) OFET mobility respectively.

$$r_{sat} = \left[\frac{\sqrt{|I_{DS}|^{max}} - \sqrt{|I_{DS}|^{0}}}{|V_{GS}|^{max}}\right]^2 \Big/ \left[\frac{WC_i}{2L}\ \mu_{sat}\right]_{calculate} \quad \textbf{(2)}$$

$$= \left[\frac{\sqrt{|I_{DS}|^{max}} - \sqrt{|I_{DS}|^{0}}}{|V_{GS}|^{max}}\right]^2 \Bigg/ \left[\frac{\partial\sqrt{|I_{DS}|}}{V_{GS}}\right]^2_{calculate} \quad \textbf{(3)}$$

$|I_{DS}|^{max}$ is the maximum drain–source current experimentally achieved at the maximum gate-source voltage $|V_{GS}|^{max}$ and $|I_{DS}|^{0}$ represents the drain–source current at V_{GS}= 0. The reliability factor gives information about the mobility (and transfer curves) that how far it is from the expected real value and how much spurious contribution is there in the transfer curve and the mobility [14]. Hence, for the critical assessment of the mobility extracted from the three slopes, values of reliability factor, r, were also calculated in order to get the effective mobility values of our devices that represent the equivalent electrical performance [14].

The effective mobility μ_{eff} is calculated from reliability factor when r =100%, using the relation (4);

$$\mu_{eff} = r \times \mu_{claimed} \quad \textbf{(4)}$$

Table 1 lists the effective and calculated mobility values on average for 8 devices as a function of storage time. **Fig. 2(b)** shows the behavior of the transfer curves with a 10 days gap when the device was stored in an ambient air conditions for 60 days. These transfer curves were used to determine the device performance parameters as a function of ambient storage time such as mobility, threshold voltage and on/off current ratios as plotted in **Fig. (3)**. To probe the changes in the film, an FTIR spectrum in the Attenuated Total Reflection (ATR) mode was performed as a function of time (**Fig. 2(c and d)**. The graph shows the transmission as a function of the wave number. The relative changes in the extracted values of mobility ($\Delta\mu_{sat}$) from the first day are given in **Fig. 3(a)**. In all the three slope regions, relatively large deviations in the mobility values were observed for the first couple of weeks. The changes started to decrease as the storage time is further increased and mobility values saturated. The relative changes in threshold voltage,

ΔV_{th} as a function of storage time are shown on the right y-axis in **Fig. 3(b)**. The relative change ($\Delta V_{th}= V_t - V_o$) is the difference in the threshold voltage values for the storage time and at the beginning of the experiment. It shows some fluctuations in ΔV_{th}, during the first couple of weeks. The relative change in ΔV_{th} has decreased as the storage time is increased. The values of on/off current ratios are shown on the left y-axis in **Fig. 3(b)**. There is on average improvement in the on/off current that shows less deviation after first few weeks. The on/off current ratio was on average around ~10^6. A surge in the on/off current ratio is observed around 10 days of storage time. We speculate that the surge in the on/off ratio around 10 days corresponds to the maximum moister absorption peak in the FTIR spectra as shown in Fig. 2 (c and d). The additional charge traps created by the water/polymer interaction lowers the off-state current, which gives rise to the on/off ratio. But as soon the water absorption tends to saturate there is not much change in on/off is observed The normalized maximum drain current with respect to the first day value, I_{dmax} as a function of storage time is plotted for $V_G=V_{DS}$=-80V in **Fig. 3(c)**. It initially showed fast decrease in the current that decayed by about 20% and then became stable and saturated with the further storage time. The performance parameters in the **Fig. 3** indicate that the OFET device showed instabilities initially and then became relatively stable after first couple of weeks.

Table 1 lists the calculated mobility, effective mobility and the reliability factor values in the three slope regions for the 60 days storage time. The values are averaged over for 8 devices with standard deviation. For each calculated value of the mobility, the reliability factor and the effective mobility is also calculated according to the equations (2), (3) and (4). The effective mobility for all the three slopes is ~0.2 cm^2/V.s. However, the calculated mobilities are different for the three slope regions. The region with the higher slope (lower gate voltage) exhibited relatively large differences between the calculated and effective mobility values and the reliability factor is also much lower than 100%. It indicates the overestimated mobility. The other two regions namely lower slope region (higher gate voltage) and the single slope region showed less difference in the calculated and the effective mobility values and hence the reliability factor is relatively better and close to 100% especially for the lower slope region. It means for our case the mobility values in the lower slope region give us more realistic values. It shows that the calculated values are not very far off the effective and realistic mobility values. It also means that the effective mobility does not depend on the exact slope of the transfer curve.

Our analysis of the performance parameters indicates that they show relatively large fluctuations during the first couple of weeks of the storage time. As the storage time increases, the performance parameters become stable. A maximum change of approximately 0.25 cm^2/V.sec, 0.13 cm^2/V.sec and 0.1 cm^2/V.sec was observed in the initial mobility values calculated from higher slope region (black line), lower slope region (red line) and the single slope region (blue line) respectively (**Fig. 3(a)**). A general trend seen from the mobility changes is that there are fluctuations or continuous changes in the mobility values for the first few weeks that gradually become stable later on as the storage time is increased. In the same way, a relatively large changes in the on/off current ratios and V_{th} values are observed that becomes relatively stable with the passage of storage time (**Fig. 3(b)**). Similarly, a large decrease is observed in the maximum drain current for the first few weeks that becomes stable with the passage of storage time of the devices (**Fig. 3(c)**).

In order to probe the reasons for the initial degradation and then stability in the OFET performance parameters later on with the storage time, we performed FTIR analysis of the films that showed moisture adsorption from the air that penetrates into the channel layer with the storage time as shown in the **Fig. 2(c)**. The DPPDTT/PMMA films were deposited on a glass substrate and the FTIR spectra were taken in the Attenuated Total Reflection (ATR) mode. There is negligible OH peak at around 3400 cm^{-1} for the freshly prepared samples but as the devices were stored in an ambient condition for an extended time period, an OH peak appears that grows in intensity and then broadens with the passage of time. This peak in the FTIR spectrum is a typical signature of water adsorption and penetration into the films. The absorbed moisture molecules have an interaction with the channel polymer layer. The interaction of OH group with the polymer is shown in **Fig. 2(d)**. The C-OH stretch band that shows the interaction of moisture with the DPPDTT is indicated with an arrow [29,30]. At day 1 there was no C-OH stretch band and it appears with the passage of time and then again disappears with the further storage that yield stable devices with the initial degradations in the polymer film. It means the initial changes in the performance parameters of the OFET are caused by the moister adsorption on the OFET films that degrade the film quality and hence the electrical performance parameters. The OH peak initially becomes more intense with the passage of time that shows more adsorption of the moisture with the passage of time. It also shows proportionate interaction with the DPPDTT as shown in **Fig. 2(d)**. The maximum deviations in the OFET parameters correspond to the

maximum intensity peak for OH in **Fig. 2(c)** (green curve for 10 day time). For long enough storage time, the OH peak becomes very broad and ultimately saturates. The distinct C-OH peak is barely visible for long enough times. The weakening interaction of OH with the polymer bonds ultimately makes the OFET parameters stable. The adsorbed water molecules at this stage must have reached saturation that caused the peak to broaden. The FTIR spectrum is consistent with the observed OFET performance parameters like mobility, threshold voltage, on/off current ratio and the threshold voltage. The maximum deviation in the performance parameters is for almost the same storage time when there is maximum intensity peak in the FTIR spectrum. It is worth mentioning that the PMMA dielectric layer that we have used is hydrophilic in nature and it could also have contributed to the water absorption to the dielectric-semiconductor interface although the adsorption must have initiated through the top polymer layer.

Conclusion:

In summary, bottom gate top contact solution-processed DPPDTT based OFET devices were fabricated and characterized for their electrical performance in the ambient environment to test their shelf life and stability. These polymer OFETs showed the charge carrier mobility, threshold voltage and current on/off ratios in the range of 0.2 $cm^2V^{-1}s^{-1}$, -15V and 10^6 respectively. The ambient atmosphere deteriorated the performance parameters and caused instabilities initially but after that the device operation became stable and negligible changes in device performance parameters were observed. The FTIR spectrum confirmed that the initial decrease in device performance is caused by the moisture adsorption and penetration into the active organic conductive layer. The stable behavior of the devices after the initial degradations suggests that the water adsorption and penetration into the organic film saturates after the first few weeks and hence further degradation in the film stops resulting in the device stability. At this stage, the interaction of moisture with the polymer shows no significant peak in the FTIR spectra that gives stability to the OFET performance parameters. Our results show that it is possible to make the OFET devices stable by aging them in the ambient conditions for couple of weeks. The demonstrated unique approach to make the OFETs stable in the ambient condition by aging will contribute to the efforts to make organic devices stable for the practical applications.

Conflict of Interest

There are no conflicts of interest to declare.

Acknowledgement

We acknowledge the stimulating discussions with Mohsin Raza, Fatima Irshad, Kashif Saghir and Hassan Farooq. We also acknowledge the financial support provided by the Higher Education Commission (HEC) of Pakistan.

References

[1] H.T. Yi, M.M. Payne, J.E. Anthony, V. Podzorov, Ultra-flexible solution-processed organic field-effect transistors, Nat. Commun. 3 (2012) 1259.
[2] T. Sekitani, U. Zschieschang, H. Klauk, T. Someya, Flexible organic transistors and circuits with extreme bending stability, Nat. Mater. 9 (2010) 1015.
[3] C. Di, F. Zhang, D. Zhu, Multi-Functional Integration of Organic Field-Effect Transistors (OFETs): Advances and Perspectives, Adv. Mater. 25 (2013) 313–330.
[4] R.A. Street, Thin-Film Transistors, Adv. Mater. 21 (2009) 2007–2022.
[5] R. Tinivella, V. Camarchia, M. Pirola, S. Shen, G. Ghione, Simulation and design of OFET RFIDs through an analog/digital physics-based library, Org. Electron. 12 (2011) 1328–1335.
[6] D.K. Hwang, C. Fuentes-Hernandez, J.B. Kim, W.J. Potscavage Jr, B. Kippelen, Flexible and stable solution-processed organic field-effect transistors, Org. Electron. 12 (2011) 1108–1113.
[7] H. Sirringhaus, Device physics of solution-processed organic field-effect transistors, Adv. Mater. 17 (2005) 2411–2425.
[8] A. Tixier-Mita, S. Ihida, B.-D. Ségard, G.A. Cathcart, T. Takahashi, H. Fujita, H. Toshiyoshi, Review on thin-film transistor technology, its applications, and possible new applications to biological cells, Jpn. J. Appl. Phys. 55 (2016) 04EA08.
[9] Y. Guo, G. Yu, Y. Liu, Functional Organic Field-Effect Transistors, Adv. Mater. 22 (2010) 4427–4447.
[10] K. Fukuda, K. Hikichi, T. Sekine, Y. Takeda, T. Minamiki, D. Kumaki, S. Tokito, Strain sensitivity and durability in p-type and n-type organic thin-film transistors with printed silver electrodes, Sci. Rep. 3 (2013) 2048.
[11] H. Sirringhaus, 25th Anniversary Article: Organic field-effect transistors: the path beyond amorphous silicon, Adv. Mater. 26 (2014) 1319–1335.
[12] J. Li, Y. Zhao, H.S. Tan, Y. Guo, C.-A. Di, G. Yu, Y. Liu, M. Lin, S.H. Lim, Y. Zhou, A stable solution-processed polymer semiconductor with record high-mobility for printed transistors, Sci. Rep. 2 (2012) 754.
[13] M.U. Chaudhry, K. Muhieddine, R. Wawrzinek, J. Li, S.-C. Lo, E.B. Namdas, Nano-Alignment in Semiconducting Polymer Films: A Path to Achieve High Current Density and Brightness in Organic Light Emitting Transistors, ACS Photonics. (2018).
[14] H.H. Choi, K. Cho, C.D. Frisbie, H. Sirringhaus, V. Podzorov, Critical assessment of charge mobility extraction in FETs, Nat. Mater. 17 (2017) 2.

[15] E.G. Bittle, J.I. Basham, T.N. Jackson, O.D. Jurchescu, D.J. Gundlach, Mobility overestimation due to gated contacts in organic field-effect transistors, Nat. Commun. 7 (2016) 10908. doi:10.1038/ncomms10908.
[16] I. McCulloch, A. Salleo, M. Chabinyc, Avoid the kinks when measuring mobility, Science. 352 (2016) 1521–1522.
[17] S. Hoshino, M. Yoshida, S. Uemura, T. Kodzasa, N. Takada, T. Kamata, K. Yase, Influence of moisture on device characteristics of polythiophene-based field-effect transistors, J. Appl. Phys. 95 (2004) 5088–5093.
[18] L.A. Majewski, J.W. Kingsley, C. Balocco, A.M. Song, Influence of processing conditions on the stability of poly(3-hexylthiophene)-based field-effect transistors, Appl. Phys. Lett. 88 (2006) 222108. doi:10.1063/1.2208938.
[19] L.A. Majewski, A.M. Song, Extended storage time of poly(3-hexylthiophene) field-effect transistors via immersion in common solvents, J. Appl. Phys. 102 (2007) 074515. doi:10.1063/1.2785011.
[20] Y. Qiu, Y. Hu, G. Dong, L. Wang, J. Xie, Y. Ma, H2O effect on the stability of organic thin-film field-effect transistors, Appl. Phys. Lett. 83 (2003) 1644–1646. doi:10.1063/1.1604193.
[21] D. Li, E.-J. Borkent, R. Nortrup, H. Moon, H. Katz, Z. Bao, Humidity effect on electrical performance of organic thin-film transistors, Appl. Phys. Lett. 86 (2005) 042105. doi:10.1063/1.1852708.
[22] Y. Sun, X. Lu, S. Lin, J. Kettle, S.G. Yeates, A. Song, Polythiophene-based field-effect transistors with enhanced air stability, Org. Electron. 11 (2010) 351–355. doi:10.1016/j.orgel.2009.10.019.
[23] T. Nishi, K. Kanai, Y. Ouchi, M.R. Willis, K. Seki, Evidence for the atmospheric p-type doping of titanyl phthalocyanine thin film by oxygen observed as the change of interfacial electronic structure, Chem. Phys. Lett. 414 (2005) 479–482. doi:10.1016/j.cplett.2005.08.113.
[24] R. Ahmed, C. Simbrunner, G. Schwabegger, M.A. Baig, H. Sitter, Air stability of C60 based n-type OFETs, Synth. Met. 188 (2014) 136–139. doi:10.1016/j.synthmet.2013.12.007.
[25] T. Someya, H.E. Katz, A. Gelperin, A.J. Lovinger, A. Dodabalapur, Vapor sensing with α,ω-dihexylquarterthiophene field-effect transistors: The role of grain boundaries, Appl. Phys. Lett. 81 (2002) 3079–3081. doi:10.1063/1.1514826.
[26] H.-I. Un, P. Cheng, T. Lei, C.-Y. Yang, J.-Y. Wang, J. Pei, Charge-Trapping-Induced Non-Ideal Behaviors in Organic Field-Effect Transistors, Adv. Mater. 30 (2018) 1800017. doi:10.1002/adma.201800017.
[27] A. Ortiz-Conde, F.J. García-Sánchez, J. Muci, A.T. Barrios, J.J. Liou, C.-S. Ho, Revisiting MOSFET threshold voltage extraction methods, Microelectron. Reliab. 53 (2013) 90–104.
[28] M.C. Hamilton, S. Martin, J. Kanicki, Field-effect mobility of organic polymer thin-film transistors, Chem. Mater. 16 (2004) 4699–4704.
[29] M. Septiyanti, Y. Meliana, E. Agustian, Effect of citronella essential oil fractions as oil phase on emulsion stability, in: Jakarta, Indonesia, 2017: p. 020070. doi:10.1063/1.5011927.
[30] A. Ghysels, V. Van Speybroeck, E. Pauwels, S. Catak, B.R. Brooks, D. Van Neck, M. Waroquier, Comparative study of various normal mode analysis techniques based on partial Hessians, J. Comput. Chem. (2009) NA-NA. doi:10.1002/jcc.21386.

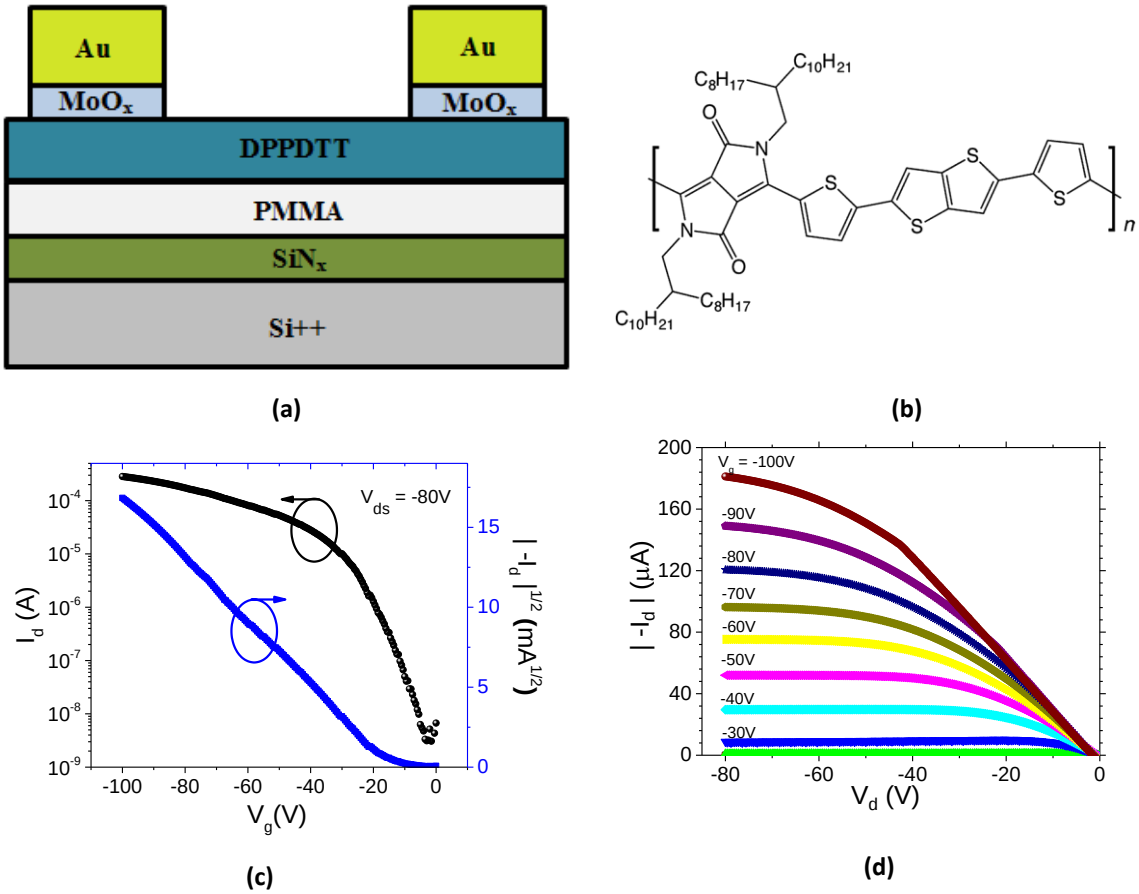

Fig. 1. (a) Schematic representation of the OFET configuration which shows different layers deposited on highly doped silicon substrate **(b)** Chemical structure of DPPDTT **(c)** Transfer characteristics of the device taken right after fabrication and **(d)** corresponding output characteristics of the device.

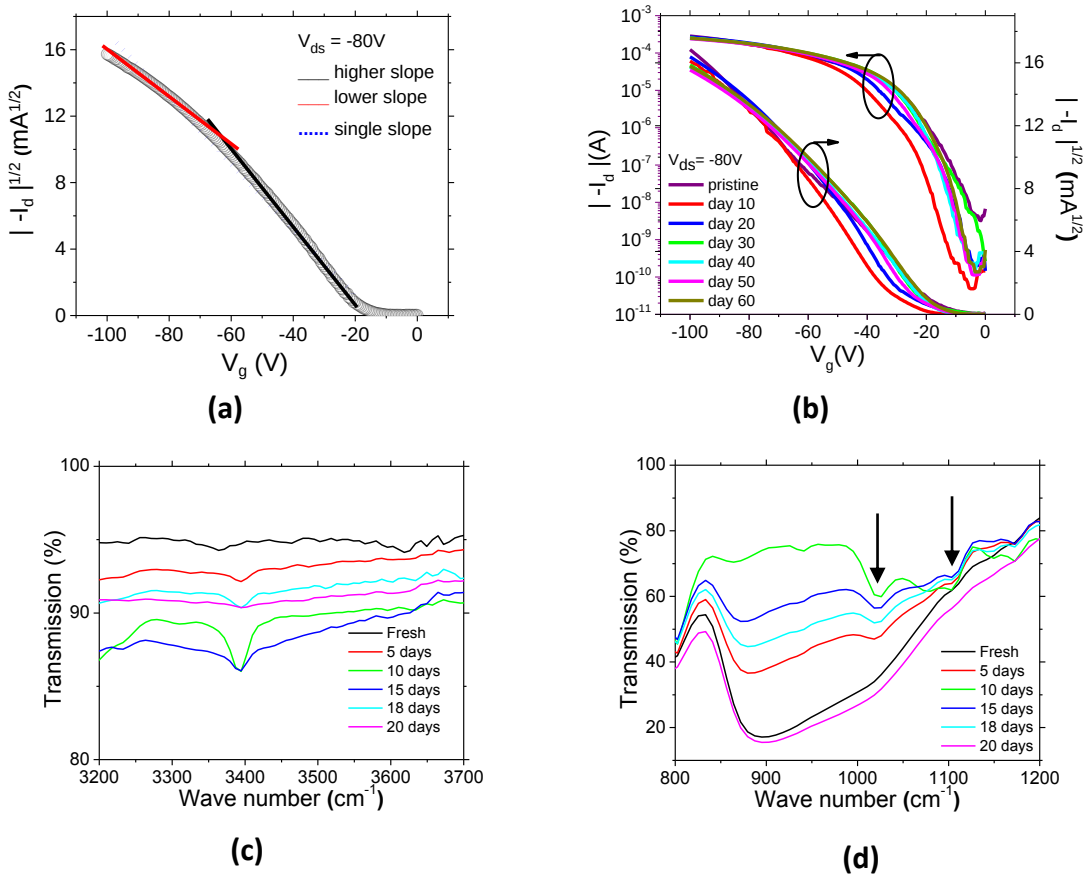

Fig. 2. Transfer characteristics (I_d vs. V_g) of the OFET device in the saturation regime at V_{SD}= -80 **(a)** Different slopes taken for mobility calculations on a transfer curve. **(b)** Transfer curves of the OFETs characterized over 60 days which shows a small variation in off-state current and threshold voltage compared to the day 1. **(c)** ATR mode FTIR spectra of PMMA/DPPDTT film as a function of storage time in the ambient air conditions. The OH peak around 3400 cm^{-1} shows the water adsorption in the film that becomes intense and broadens with the passage of storage time. **(d)** The FTIR spectra that shows the interaction of OH with the polymer material. The arrows show the bands for C-OH stretching at a wavenumber 1026 cm^{-1} and 1103 cm^{-1}.

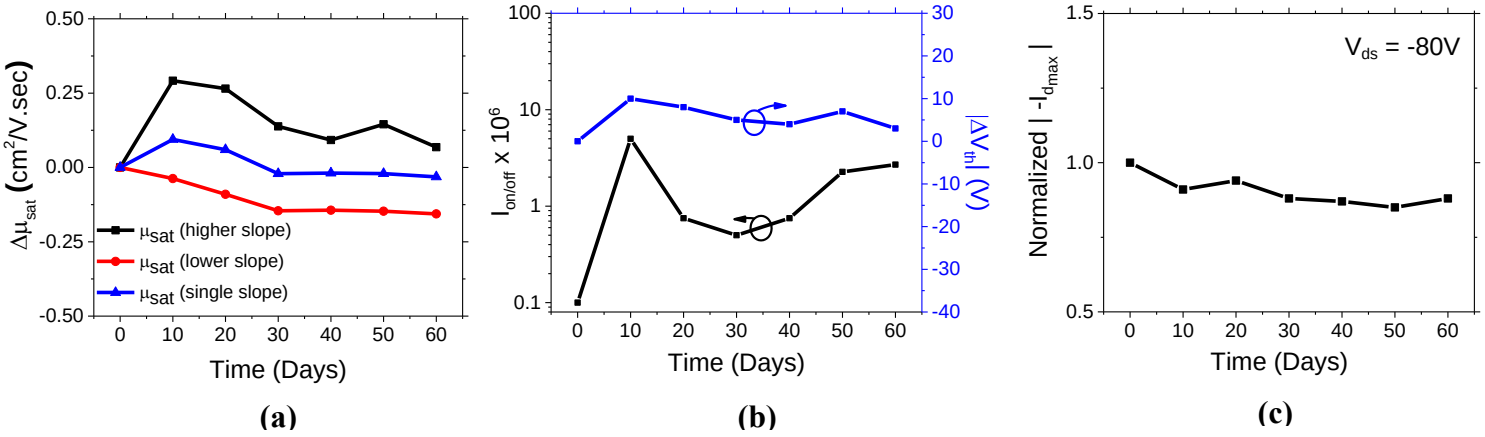

Fig. 3. Shelf life stability parameters for the device, stored and characterized for 60 days in an ambient air environment **(a)** The relative changes in the hole mobility for three different slopes calculated for 60 days in an ambient air shows a little deviation from the mobility values right after fabrication for the first few weeks and then stabilize. The mobilities were calculated for three regions on the transfer curves- higher slope region, lower slope region and full curve slope **(b)** The on/off current ratio shows improvement when stored for a long period and threshold voltage change also shows stability in device performance at ambient environment **(c)** Normalized current behavior in I_{dmax} of the device shows a slight decrease for about 30 days and then steady behavior after being stored at room temperature in the ambient air conditions for 60 days.

Time after first characterization	μ_{sat}(cm^2/V.sec)								
	Higher slope			Lower slope			Single slope		
	μ_{cacl}	r_{sat}%	μ_{eff}	μ_{cacl}	r_{sat}%	μ_{eff}	μ_{cacl}	r_{sat}%	μ_{eff}
0 day	0.32±0.02	63±6	0.20±0.02	0.29±0.04	71±2	0.20±0.02	0.3±0.01	68±4	0.20±0.02
10 days	0.61±0.08	34±1	0.20±0.01	0.26±0.04	76±5	0.20±0.01	0.43±0.03	55±6	0.20±0.01
20 days	0.63±0.06	34±2	0.21±0.01	0.21±0.02	99±10	0.21±0.01	0.38±0.01	57±2	0.21±0.01
30 days	0.43±0.01	40±4	0.20±0.01	0.19±0.07	110±4	0.20±0.01	0.31±0.04	64±6	0.20±0.01
40 days	0.40±0.05	46±1	0.18±0.02	0.18±0.01	103±10	0.19±0.01	0.29±0.01	65±3	0.20±0.01
50 days	0.50±0.04	38±3	0.19±0.01	0.16±0.02	123±19	0.19±0.01	0.27±0.03	73±10	0.19±0.01
60 days	0.37±0.07	55±7	0.19±0.01	0.15±0.03	124±7	0.20±0.02	0.24±0.05	74±5	0.20±0.02

Table 1: The table shows the average calculated and effective mobility values in the three slope regimes for the DPPDTT based OFET device analyzed for the 60 days storage time in the ambient air conditions. The reliability factor, r, is also calculated that gives indication that how far or close the calculated mobility values are from the ideal transistor behavior without any spurious and unreal effects.